BLIND ESTIMATION OF PIXEL BRIGHTNESS TRANSFORM

Xing Zhang and Siwei Lyu

Computer Science Department
University at Albany, State University of New York

ABSTRACT

Pixel brightness transforms (PBT), examples of which include gamma correction, sigmoid stretching and histogram equalization, are common operations on digital images, and it is practically useful to estimate such transforms directly from an image. In this work, we describe an effective and efficient method to estimate PBT from images, which takes advantage of the nature of PBT as a mapping between integral pixel values and the distinct characteristics it introduces to the pixel value (PV) histograms of the transformed image. Our method recovers the original PV histogram and the PBT simultaneously with an efficient iterative algorithm, and can effectively handle perturbations due to noise and compression. We perform experimental evaluation to demonstrate the efficacy and efficiency of the proposed method.

Index Terms— blind estimation, pixel brightness transform, pixel histogram

1. INTRODUCTION

The integral pixel values in a digital image do not directly reflect the amount of light projected on the camera sensor at the time of capture. Such is mainly due to the two mappings in the imaging process. First, the continuous scene radiance x is mapped to raw integral pixel value $j = \psi(x)$ with the camera response function (CRF). Subsequently the raw pixel values may further undergo the Pixel brightness transform (PBT) to become the final integral pixel value $i = \phi(j)$. Examples of PBT include gamma correction, sigmoid stretching or histogram equalization [**?**].

From the practical point of view, blind estimation of PBT from a single image is useful for two main reasons. First, it can help to correct nonlinearity applied to integral pixel values, and thus facilitates radiometric calibration and other computer vision applications, such as image registration, matching and retrieval, that predicate on raw pixel values. Second, in forensic analysis of digital images [**?**], recovering PBT can be used to reconstruct the processing history of an image in establishing its authenticity, or to differentiate regions from different source images in detecting tampering.

There have been only a few previous works addressing this problem. As the most common PBT, several works have focused on the blind estimation of gamma correction. The method in [**?**] uses higher order statistical dependencies introduced by gamma. The method of [**?**] uses the the features developed in [**?**] to recover the actual gamma value by applying different gamma values to a uniform histogram and identifying the optimal value that best matches the observed PV histogram features. Using a set of features characterizing the shapes of PV histogram after a PBT, the work in [**?**] develops method to determine if an image has undergone gamma correction or histogram equalization, but this method cannot recover the actual transform. The work [**?**] describes an iterative algorithm to jointly estimate a nonparametric PBT and the PV histogram of the original image, based on a probabilistic model of PV histogram and an exhaustive matching procedure to determine which histogram entries are most likely to correspond to artifacts caused by the PBT. Last, there are recent works (e.g., [**?**]) to recover the whole image processing pipeline including PBT blindly from images.

In this work, we describe an effective and efficient method to estimate PBT from a single image. This method takes advantage of the special nature of PBT as a mapping between integral pixel values that introduces distinct characteristics to the pixel value (PV) histograms of the transformed image. It recovers the original PV histogram and the PBT simultaneously with an efficient iterative algorithm. We show experimental results demonstrating the efficacy and efficiency of our method.

2. PBT AND ITS EFFECT ON PV HISTOGRAM

For simplicity, we focus our discussion on gray-scale images whose pixel values are encoded with b-bits that correspond to $N = 2^b$ different values. Most PBTs can be modeled as a continuous mapping followed by a rounding operation that maps real value back to integers[1]. Specifically, each input pixel value, $j \in \{0, \cdots, N-1\}$, is mapped to its corresponding output pixel value, $i \in \{0, \cdots, N-1\}$, as $i = \phi(j) := \text{round}[m(j)]$, where $m(\cdot) : [0, N-1] \mapsto [0, N-1]$ is a continuous transform. Furthermore, most forms of $m(\cdot)$ of practical interest is monotonic, which we will assume subse-

[1] Other operations recovering integer values from continuous values such as `floor` or `ceiling` can also be used.

quently. Examples of $m(\cdot)$ include

- gamma correction,

$$m_\gamma(j) = N\left(\frac{j}{N}\right)^\gamma, \tag{1}$$

- sigmoid stretching

$$m_{\alpha,\beta}(j) = N\left(1+\exp\left(\frac{\beta-\frac{j}{N}}{\alpha}\right)\right)^{-1}, \tag{2}$$

- histogram equalization,

$$m(j) = \rho^{-1}\left(\frac{j}{N}\right), \tag{3}$$

  where $\rho^{-1}(\cdot)$ is the interpolated inverse cumulative density function of the pixels of the input image,
- free-form intensity transform, such as the `curves` tool in Adobe Photoshop.

The first two are examples of parametric PBT and the latter two are nonparametric PBTs. It should also be pointed out that even though $m(\cdot)$ is invertible, the overall PBT in general may not be invertible due to the rounding step.

Because of its Pixel nature, we can understand the effect of PBT on an image by examining the pixel value (PV) histogram. Specifically, we have

$$\mathcal{P}_{\text{output}}(i) - \sum_{j=0}^{N-1}\delta\left(i=\text{round}[m(j)]\right)\cdot\mathcal{P}_{\text{input}}(j). \tag{4}$$

For convenience, we normalize the PV histogram to have a unit total sum, so it can be treated as a probability distribution over pixel values. We represent the normalized PV histograms of the input and output image as vectors on the N-dimensional probability simplex, such that $x_j = \mathcal{P}_{\text{input}}(j-1)$ and $y_i = \mathcal{P}_{\text{output}}(i-1)$, and introduce matrix H that is defined as $H_{ij} = \delta\left(i-\text{round}[m(j-1)]+1\right)$, for $i,j \in \{1,\cdots,N\}$, then Eq.(**??**) can be rewritten as $y_i = \sum_{j=1}^{N} H_{ij}x_j$, or in the more compact matrix and vector form, as:

$$\mathbf{y} = H\mathbf{x}. \tag{5}$$

For PBT that is not identity, there will be multiple input pixel values map to a single output pixel value, and output pixel values to which no input pixel value maps based on the pigeonhole principle [**?**]. This redistribution of pixel values creates peaks and gaps in the shape of the output PV histogram, which is illustrated in two cases (gamma correction and histogram equalization) in the second and third rows of Fig.**??**. In contrast, the PV histogram of typical photographic image not undergoing PBT is more smooth (first row Fig.**??**). The difference in smoothness of these PV histograms can be better revealed with the first order difference of the values of neighboring bins, as shown in the last column of Fig.**??**. Note that when measured with the ℓ_1 norm, the first order difference of neighboring components for the PV histogram of the original image is considerably smaller than those of images undergone PBTs[2].

[2]Similar regularities of PV histograms have also been observed on a wide range of other photographic images.

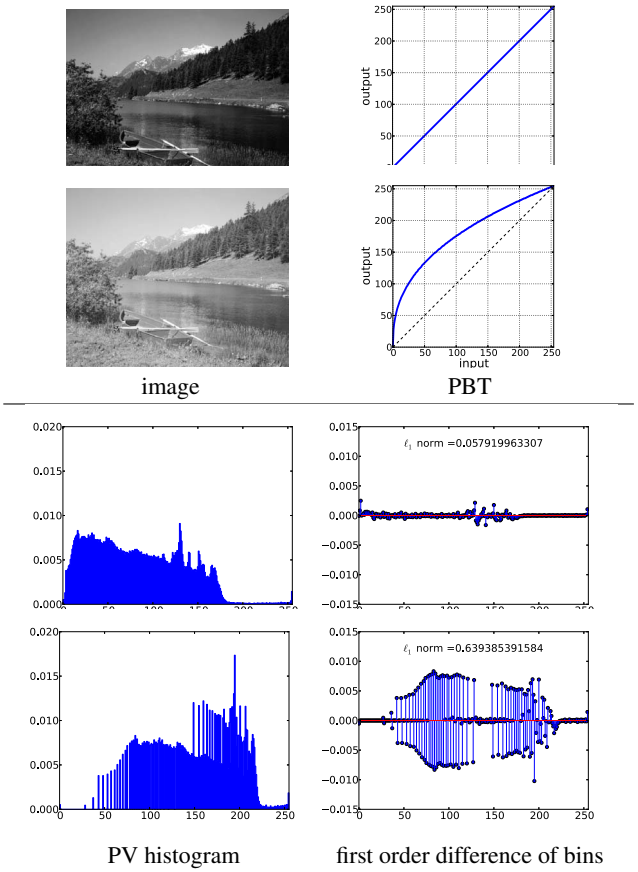

Fig. 1: *Effects of Pixel brightness transform (PBT) on a photographic image and its pixel value (PV) histogram. The three rows in the top panel correspond to the three rows in the bottom.*

3. ESTIMATING PBT FROM IMAGE

The central problem in PBT estimation is to recover the transform and the vectorized PV histogram $\mathbf{x}$ of the input image using only the vectorized PV histogram of an image undergone PBT, $\mathbf{y}$. More specifically, this is to solve for H and $\mathbf{x}$ simultaneously in Eq.(**??**) with known $\mathbf{y}$.

3.1. Recovering Original PV Histogram

The problem of recovering $\mathbf{x}$ from $\mathbf{y}$ and H is oftentimes ill-posed – unless matrix H is identity, it contains rows of all zeros corresponding to output pixel values to which no input pixel value maps.

To obtain a stable solution, we need to enforce more constraints on the values of $\mathbf{x}$. As results in Fig.**??** suggest, we formulate the problem of estimating $\mathbf{x}$ as an ℓ_1 constrained least squares problem – we seek the optimal $\mathbf{x}$ that leads to "similar" PV histogram to $\mathbf{y}$ measured by the ℓ_2 difference, and has small ℓ_1 norm for the first order differences of neighboring components. Formally, this is expressed with the following constrained optimization problem:

$$\min_{\mathbf{x},\text{s.t.}\mathbf{1}^T\mathbf{x}=1,\mathbf{x}\geq 0}\ \tfrac{1}{2}\|\mathbf{y}-H\mathbf{x}\|_2^2+\lambda\|D\mathbf{x}\|_1 \tag{6}$$

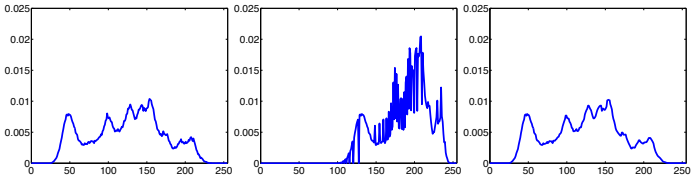

Fig. 2: *Recovery of the PV histogram of an* 8*-bit grayscale image that has been gamma corrected with* $\gamma = 0.4$ *(the corresponding matrix* H *has a rank of* 176 *out of a full rank of* 256*).* **(left)** *original PV histogram.* **(middle)** *observed PV histogram after gamma correction.* **(right)** *recovered PV histogram.*

where $\lambda \geq 0$ is a system parameter that controls the tradeoff between the ℓ_2 and ℓ_1 losses. Matrix D corresponds to the first order discrete difference operator. We will refer to the optimal value of the objective function of (**??**) as $L^\star(H, \lambda)$. The optimization problem in (**??**) is convex, and it can be solved with general-purpose convex programming package such as CVX [**?**, **?**]. Shown in Fig.**??** is an example of the recovery of the PV histogram of an 8-bit grayscale image undergone a gamma correction with $\gamma = 0.4$ (the corresponding matrix H has a rank of 176 out of a full rank of 256). As the result shows, the recovered PV histogram is very close to the original PV histogram, and the presence of small flat regions are the results of the smoothness penalty.

3.2. Recovering Pixel Brightness Transform

We now turn to the problem of estimating the original PV histogram $\mathbf{x}$ and transformation matrix H simultaneously. We discuss two cases: (i) parametric PBT specified with a small number of parameters and (ii) nonparametric PBT as a mapping for every possible input in $\{0, \cdots, N-1\}$.

Parametric PBT. We have consistently observed that the true transform parameter usually corresponds to a global minimum of the objective function of (**??**) over a range of values. For instance, Fig.**??** shows the values of $L^\star(H(\gamma), \lambda)$ corresponding to gamma correction PBT, Eq.(**??**), with $\gamma \in [0.1, 1.8]$ ($\lambda = 0.1$ is fixed in all cases). The two curves shown correspond to $\gamma = 0.4$ and 1.4, respectively, where the true parameter values lead to global minimums of $L^\star(H(\gamma), \lambda)$ as shown by the red circles[3].

Based on this observation, our method of finding the optimal PBT parameter is based on solving

$$\gamma^\star = \operatorname*{argmin}_{\gamma} L^\star(H(\gamma), \lambda), \tag{7}$$

where we use $H(\gamma)$ to make explicit the dependence of matrix H on parameter γ. This objective function is not differentiable with regards to γ due to the rounding step. Yet, when the PBT can be specified by one or two parameters, we found a simpler approach, which first performs a grid search in a given range of parameter values followed by a binary search between the reduced ranges where overall values of $L^\star(H(\gamma), \lambda)$ is minimal, is usually effective and leads to satisfactory solutions to (**??**).

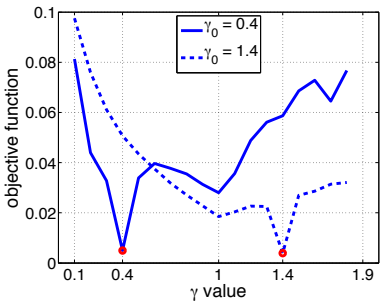

Fig. 3: *The relation between the value of* $L^\star(H(\gamma), \lambda)$ *and* γ *values, in the case of PBT in the form of simple gamma correction. The true* γ *value in the two cases are* 0.4 *and* 1.4*, which correspond to the global minima of the two curves.*

Nonparametric PBT. When the PBT cannot be specified with a parametric form, we estimate the PBT directly and recover the original PV histogram simultaneously. This is achieved with an iterative method: starting with initial values for H and $\mathbf{x}$, we iterate between (i) solving for $\mathbf{x}$ with fixed H and (ii) solving H with fixed $\mathbf{x}$. The former is solved with the steps described in Section **??**, and we turn to the solution of the latter here. Specifically, with the vectorized input and output PV histograms $\mathbf{x}$ and $\mathbf{y}$, it can be shown that a unique deterministic monotonic transform exists that satisfies (i) it converts a variable with distribution given by $\mathbf{x}$ to another that has distribution given by $\mathbf{x}$, and (ii) it minimizes the overall work that is measured by the total displacement of bins[4]. This transform is obtained by *histogram matching*.

Formally, denote $\chi_{\mathbf{x}}(\cdot) : \{0, N-1\} \mapsto [0, 1]$ and $\chi_{\mathbf{y}}(\cdot) : \{0, N-1\} \mapsto [0, 1]$ as the cumulative density functions induced from $\mathbf{x}$ and $\mathbf{y}$, respectively, i.e., $\chi_{\mathbf{x}}(i) = \sum_{k=1}^{i} \mathbf{x}_i$ and $\chi_{\mathbf{x}}(i) = \sum_{k=1}^{i} \mathbf{y}_i$. and $\chi_{\mathbf{y}}^{-1}(\cdot) : [0, 1] \mapsto \{0, N-1\}$ as the pseudo inverse cumulative distribution induced from $\mathbf{y}$, as $\chi_{\mathbf{y}}^{-1}(p) = i$ if $\chi_{\mathbf{y}}(i-1) < p \leq \chi_{\mathbf{y}}(i)$. Then the mapping satisfying the two aforementioned conditions is given by [**?**]

$$f(i) = \chi_{\mathbf{y}}^{-1}(\chi_{\mathbf{x}}(i)), \tag{8}$$

and the corresponding transform matrix is obtained as $H_{ij} = \delta(j = f(i))$.

In summary, our algorithm iterates between optimizing $\mathbf{x}$ with (**??**) and computing mapping from histogram matching with Eq.(**??**). While we have not obtain a theoretical proof of convergence, in practice we observe that the algorithm usually converges within less than 10 iterations. Fig.**??** demonstrate the convergence of one estimated PBT, with the original PBT obtained from cubic spline interpolation of key points that are chosen manually. As it shows, after 5 iterations of the algo-

[3] Similar observations have also been made on other types of parametric PBTs, such as sigmoid stretching and cubic spline curves.

[4] This is a direct corollary of the optimal transportation plan on the real line in the Monge-Kantorovich transportation theory framework [**?**].

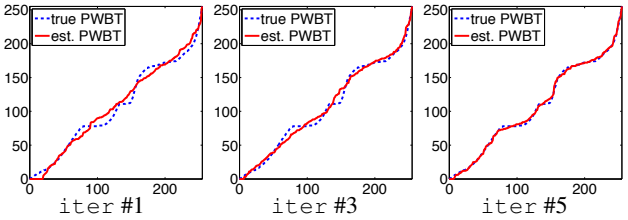

Fig. 4: *Convergence of the estimated nonparametric free-form PBT using our algorithm.*

actual γ	estimated γ (mean/std)		
	our method	method of [**?**]	method of [**?**]
0.20	0.21 (0.01)	0.26 (0.04)	0.24 (0.04)
0.60	0.60 (0.01)	0.55 (0.17)	0.58 (0.16)
1.00	1.00 (0.00)	1.15 (0.64)	1.00 (0.01)
1.40	1.40 (0.02)	1.52 (0.44)	1.44 (0.16)
1.80	1.80 (0.00)	2.12 (0.11)	1.78 (0.14)
2.20	2.21 (0.01)	2.49 (0.24)	2.13 (0.08)
2.60	2.60 (0.01)	2.92 (0.42)	2.68 (0.09)

Table 1: *Performances of estimating gamma correction PBT on the* 100 *test images with different* γ *values.*

rithm, the estimated PBT is already close to the original PBT.

4. EXPERIMENTS

We perform several experiments to evaluate the described method. The data used in our experiments are 100 grayscale images from the van Hateren database [**?**]. The test images were created from the central 1024×1024 crops of the 100 original images and reduced to 8-bit pixels.

Parametric PBT We test our method on the blind estimation of several parametric PBTs, including gamma correction, Eq.(**??**), and sigmoid stretching, Eq.(**??**). The PBT transformed images are created from the 100 test images: for gamma correction, we use γ values taking from the range $[0.2, 2.8]$ with a 0.2 step; for sigmoid stretching, we choose several different combination of α and β values.

Gamma Correction. We apply our detection algorithm and compare with two previous works on blind estimation of gamma parameters [**?**, **?**]. The results, shown as the averages and standard deviations of the estimated γ value over the 100 test images, are reported in Table **??**. The estimation performance with our method is near perfect and significantly better than those of the two compared previous works.

Sigmoid Stretching. The next experiment tests the performance of our method on the estimation of parameters of sigmoid stretching, and the detection results are reported in Table **??**. To our best knowledge, there has been no previous method for this purpose. As in the case of gamma correction, our method can accurately estimate the transformation parameters (i.e., α and β).

Nonparametric PBT We further test our methods to recover two different types of nonparametric PBTs – histogram equalization (Eq.(**??**)) and free-form nonparametric PBT created by cubic spline interpolation of manually selecting key points. The latter resembles tone mapping tools in photo-editing software (e.g., the `Curve` tool in `Photoshop`). We applied histogram equalization and free-form PBTs to each of the test images, and then use the algorithm described in Section **??** to recover the integral mapping in the PBT directly. We measure the performance by the root mean squared error (RMSE) between the actual PBTs and the corresponding estimated PBTs, treating both as functions over $[0, N-1] \mapsto [0, N-1]$. We compare with the only known previous work for the same task is [**?**], which is based on an iterative and exhaustive search of PV histograms that can lead to the observed PV histogram of an image with PBT. As the results in Table **??** show, both algorithms achieve good estimation performances when there is no perturbation. However, our method on average is $5-10$ times faster in running time, because the method [**?**] relies on exhaustive search.

actual α/β	estimated α/β (mean/std)
0.5/-1.0	0.49 (0.01) /-1.02 (0.01)
0.5/ 1.0	0.50 (0.01) / 1.01 (0.02)
1.0/-1.0	0.98 (0.02) /-0.99 (0.01)
1.0/ 1.0	1.01 (0.02) / 1.04 (0.03)
2.0/-1.0	2.02 (0.03) /-0.98 (0.02)
2.0/ 1.0	1.97 (0.02) /0.98 (0.01)

Table 2: *Performances of estimating sigmoid stretching on the* 100 *test images with different* α, β *values.*

	RMSE (mean/std)	
	ours	method of [**?**]
histogram equalization	0.12 (0.06)	0.17 (0.08)
free-form PBT	0.09 (0.02)	0.14 (0.06)

Table 3: *Performance for estimation of histogram equalization and the estimation of free-form PBT. Smaller RMSE values correspond to better performances.*

5. CONCLUSION

In this work, we have described an effective method that can blindly recover Pixel brightness transforms as mappings between integral pixel intensities. Our method takes advantage of the observed smoothness of PV histograms of the untransformed digital images. We demonstrate the effectiveness of our method on a set of images and showing recovery results close to perfect. There are several extensions we would like to further study. First, the method described here can be extended to the cases of RGB color images. Furthermore, by examining local areas in the image, we will also investigate using this method for the detection of forged image regions that have undergone different PBTs.

Acknowledgment: This work is partly supported by the National Science Foundation under Grant Nos. IIS-0953373, IIS-1208463 and CCF-1319800. We also thank the anonymous reviewers for their helpful comments.

6. REFERENCES

[1] G. Cao, Y. Zhao, and R. Ni. Forensic estimation of gamma correction in digital images. In *Image Processing (ICIP), 2010 17th IEEE International Conference on*, pages 2097 –2100, sept. 2010.

[2] CVX Research Inc. CVX: Matlab software for disciplined convex programming, version 2.0 beta. http://cvxr.com/cvx, Sept. 2012.

[3] H. Farid. Blind inverse gamma correction. *IEEE Transactions On Image Processing*, 10(10), 2001.

[4] M. Gonzalez and F. Woods. *Digital image processing*. Printice Hall, 2nd edition, 2002.

[5] M. Grant and S. Boyd. Graph implementations for nonsmooth convex programs. In V. Blondel, S. Boyd, and H. Kimura, editors, *Recent Advances in Learning and Control*, Lecture Notes in Control and Information Sciences, pages 95–110. Springer-Verlag Limited, 2008. http://stanford.edu/~boyd/graph_dcp.html.

[6] R. P. Grimaldi. *Discrete and Combinatorial Mathematics: An Applied Introduction*. 4th edition, 1998.

[7] S. Kim, H. Lin, Z. Lu, S. Süsstrunk, S. Lin, and M. Brown. A new in-camera imaging model for color computer vision and its application. *IEEE Transactions on Pattern Analysis and Machine Intelligence*, 34(12):2289–2302, 2012.

[8] H. T. Sencar and N. Memon, editors. *Digital Image Forensics: There is More to a Picture than Meets the Eye*. Springer, 2012.

[9] M. Stamm and K. Liu. Forensic detection of image manipulation using statistical intrinsic fingerprints. *Information Forensics and Security, IEEE Transactions on*, 5(3):492–506, 2010.

[10] M. Stamm and K. Liu. Forensic estimation and reconstruction of a contrast enhancement mapping. In *Acoustics Speech and Signal Processing (ICASSP), 2010 IEEE International Conference on*, pages 1698 –1701, march 2010.

[11] J. van Hateren and A. van de Schaaf. Independent component filters of natural images compared with simple cells in primary visual cortex. *Proceedings: Biological Sciences*, 265(1394):359–366, 1998.

[12] C. Villani. *Optimal Transport: Old and New*. Springer, Berlin, 2008.